Catalysis Today 157 (2010) 16–23

Contents lists available at ScienceDirect

Catalysis Today

journal homepage: www.elsevier.com/locate/cattod

Using time-resolved methods to monitor and understand catalytic oxidation reactions

Evgenii V. Kondratenko *

Leibniz Institute for Catalysis at the University of Rostock, Albert-Einstein-Str. 29A, D-18059 Rostock, Germany

ARTICLE INFO

Article history:
Available online 11 February 2010

Keywords:
Transient techniques
Time-resolved catalyst characterization
Isotopic traces
Kinetics
Reaction mechanism
Heterogeneous oxidation catalysis
TAP
SSITKA

ABSTRACT

A number of strategies for time-resolved analysis of heterogeneous oxidation reactions are being explored. They comprise the temporal analysis of products (TAP) reactor including micro-kinetic evaluation of TAP experiments, steady-state isotopic transient kinetic analysis, and time-resolved catalyst characterization by in-situ spectroscopic techniques. The present review demonstrates the potential of these methods for elucidating mechanistic and kinetic aspects of oxidative functionalization of C_2–C_3 hydrocarbons, water–gas shift reaction, direct N_2O decomposition, and high-temperature ammonia oxidation to nitric oxide (Ostwald process). Particular emphasis will be put on the application of isotopic labels and time-resolved analysis of gas-phase and surface species for identifying true surface intermediate species. Perspectives in further developments of time-resolved methods will be also indicated.

1. Introduction

Catalysis affects our life in myriad ways. It provides a means of converting readily available raw materials to higher value-added products. More than 80% of all chemicals have come into contact with at least one catalyst during their manufacturing [1]. Today, the modern industry faces challenges in utilizing alternative feedstock, creating new materials, and reducing harmful by-products. New catalysts are needed to meet these requirements. However, designing new materials or improving the existing ones requires in-depth knowledge on the individual reaction pathways, active sites and their kinetic relationships. Having this information opens the possibility to alter catalyst structures in a rational way for increasing and decreasing the rates of desired and undesired elementary reaction steps, respectively. To accomplish these objectives, various approaches are applied.

Steady-state techniques are easy in use for mechanistic studies but do not provide the required fundamental knowledge on an elementary level. Deeper mechanistic information can be derived from surface science studies in ultra-high vacuum with well-defined catalytic systems [1]. Using high-performance computing hardware and software allows simulating catalytic processes over ideal catalytic systems [1]. These both approaches enhance our fundamental understanding of catalytic reactions. Unfortunately, the extrapolation of this knowledge to industrial catalysis is not always straightforward due to the broad pressure and material gaps.

Recently, different characterization techniques have been adopted for in-situ monitoring the events taking place over real catalytic materials under industrially relevant reaction conditions [2–9]. They can provide valuable insights into the nature of active species and surface intermediates. Transient kinetic techniques such as the TAP (temporal analysis of products) reactor [10–12] and SSITKA (steady-state isotopic transient kinetic analysis) [13] have the potential for clarifying complex reactions on a near to elementary level and for determining kinetic parameters of these individual steps.

The application of transient methods in heterogeneous catalysis has been well known since the 1960s. Several reviews including monographs and special issues are available [1,14–20]. This paper highlights the potential of transient kinetic techniques and time-resolved in-situ catalyst characterization for monitoring and understanding oxidation heterogeneous reactions at a near to molecular level in the last five years. Particularly, the importance of isotopic labels and high-time resolution product analysis will be stressed. It will be shown that transient kinetic studies in combination with time-resolved in-situ catalyst characterization and DFT calculations allow the understanding of selectivity- and activity-determining factors for a number of gas-phase catalytic reactions such as oxidative functionalization of C_2–C_3 hydrocarbons, water–gas shift reaction, direct decomposition of nitrous oxide, and high-temperature ammonia oxidation to nitric oxide (Ostwald process).

* Tel.: +49 381 1281290; fax: +49 381 1281 51290.
E-mail address: Evgenii.kondratenko@catalysis.de.

0920-5861/$ – see front matter © 2010 Elsevier B.V. All rights reserved.
doi:10.1016/j.cattod.2010.01.031

2. Basic principles and approaches

In transient experiments, one or more reaction parameters, like temperature, pressure or concentration of reaction components, are temporarily changed. Temporal responses of catalytic system on this change are monitored as a function of time. For analyzing gas-phase components at the reactor outlet, mass spectroscopy is generally preferred due to its fast analysis and for discriminating between isotopes. Compared to steady-state tests, transient experiments are performed with a higher time resolution then enabling detection of short-lived intermediates and unraveling complex reaction networks in terms of near to elementary reaction steps. Moreover, modern in-situ characterization techniques (e.g. IR, Raman, and UV/vis) enable to analyze catalytic materials during transient experiments. Therefore, kinetic information on surface processes can be derived from analysis of temporal changes in catalyst composition and concentration of active species.

2.1. Temperature-programmed methods

Nowadays, transient techniques like temperature-programmed reduction (TPR), oxidation (TPO) and desorption (TPD) are almost routinely used in many research laboratories [1]. Such experiments are usually performed in continuous flow fixed-bed reactors, in which temperature is programmed to rise typically in a linear fashion. Gas-phase components leaving the reactor are monitored as a function of temperature. The resulting concentration profile contains information on adsorption and desorption processes, the number and uniformity of active catalyst sites. When reaction takes place, this gives information related to the reaction rates and the reaction mechanism.

2.2. Temporal analysis of products reactor

The Temporal Analysis of Products reactor has been developed by John T. Gleaves and his team at Monsanto [21–24]. This is a pulse technique operating in vacuum ($p \sim 10^{-5}$ Pa) with very low (0.1–100 nmol/pulse) amounts of reactants [10–12]. Due to the low pulse size, isothermal operation of even highly exothermic or endothermic reactions is ensured. During pulsing the peak pressure in the micro-reactor filled with catalyst can increase up to 200 Pa [25], i.e. the TAP reactor is located between the ultra-high vacuum (UHV) and ambient pressure techniques. After leaving the micro-reactor, the non-reacted feed components and formed reaction products are analyzed by mass spectroscopy with a time resolution of 100 μs.

Together with the reactor geometry the pulse size determines the diffusion regime. When the pulse size is below 1 nmol, gas transport in the micro-reactor occurs typically via Knudsen diffusion. Operating under such conditions is a very important feature of the TAP experiments, since the collisions between gas-phase molecules are strongly minimized. Therefore, pure heterogeneously catalyzed reactions are under investigation. Transient experiments with higher pulse sizes are also very useful, because they provide important information about the influence of gas-phase reactions on the investigated heterogeneous reactions.

2.3. Isotopic transient kinetic methods

Steady-state isotopic transient kinetic analysis is one of the powerful techniques for kinetic and mechanistic analysis of reactions on the catalyst surface under real reaction conditions [13,15]. In SSITKA experiments, two feeds differing only in their isotopic composition are usually used. In the beginning, steady-state operation conditions are achieved using the feed with a common isotopic label. Hereafter, this feed is replaced by another feed containing a different isotope. As the isotopically labeled reactant progresses through the reactor and reacts on the catalyst surface to products, the new isotopic label is distributed between reaction products and unreacted reactant(s). The temporal concentration of the labeled compounds is monitored at the reactor outlet using a mass spectrometer. The resulting transients contain information on concentration of adsorbed reaction intermediates, their coverage, and surface lifetimes as well as on site heterogeneity and activity distribution. This technique has been successfully used in a number of studies to derive kinetic and mechanistic insights into different heterogeneously catalyzed reactions [1,13].

3. Possibilities of time-resolved methods in oxidation heterogeneous catalysis

3.1. Elucidating sequence of product formation

The below examples demonstrate the potential of the TAP reactor for mechanistic analysis of high-temperature ammonia oxidation to nitric oxide (Ostwald process) over industrial Pt–Rh gauzes, individual Pd, Pt, and Rh wires as well as over metal oxides [25–31]. Understanding the origins of product formation and selectivity-determining factors was possible due to the following unique features of the TAP reactor: (i) low pulse size enabling isothermal operation; (ii) smaller pressure gap between TAP experiments and industrial ammonia burners compared to ultra-high vacuum set-ups; (iii) sub-millisecond time resolution, (iv) application of isotopic labels, (v) pump-probe experiments for probing reactivity/selectivity of adsorbed species and (vi) usage of industrial or industrially relevant materials.

Fig. 1 exemplifies transient responses recorded after sequential pulsing of O_2 and $^{15}NH_3$ over Pt and Rh wires at 1073 K. The ammonia transient is not shown in this figure. The usage of $^{15}NH_3$ was very important in order to unambiguously prove the formation of nitrous oxide. From a mechanistic point of view, the results presented in Fig. 1 were interpreted as following. The sharp decrease in the oxygen transient response at 0.1 s was due to the reaction of ammonia with adsorbed oxygen species formed over noble metals in the oxygen pulse. ^{15}NO was detected directly after $^{15}NH_3$ entered the reactor. The next detected reaction product was $^{15}N_2O$ and appeared after ^{15}NO. The final product was $^{15}N_2$. Analyzing the order of appearance of these responses as well as their shapes revealed that ammonia was primarily oxidized to nitric oxide followed by its consecutive conversion with non-reacted ammonia to yield nitrous oxide and nitrogen. Rh was more reactive for these secondary transformations than Pt. DFT calculations in [30] concluded that the higher reactivity of Rh was due to: (i) higher barrier of NO formation, (ii) stronger NO adsorption and (iii) lower barrier of NO decomposition. The use of labeled ammonia ($^{15}NH_3$) was also very essential to conclude that nitrogen and nitrous oxide originated via coupling of ^{14}NO and $^{15}NH_x$ ($x = 0–2$) fragments [26,27,29]. Similar mechanistic scheme is also valid for Pt/Rh gauze [25] as well as for Fe_2O_3, Cr_2O_3, and CeO_2 [29]. Therefore, mechanistic features of ammonia oxidation over the noble metals and the oxides are similar. Non-selective conversions of nitric oxide over surface ammonia species were suppressed in the presence of gas-phase oxygen [32]. A near to 100% NO selectivity at a complete NH_3 conversion was obtained using an $O_2/NH_3 = 10$ feed [30]. Under such conditions the coverage by O species was significantly higher than that of NH_x fragments suppressing consecutive NO conversion.

3.2. Deriving micro-kinetics

The TAP reactor was often applied to derive kinetics of various oxidation reactions [12]. However, only a few studies tried to

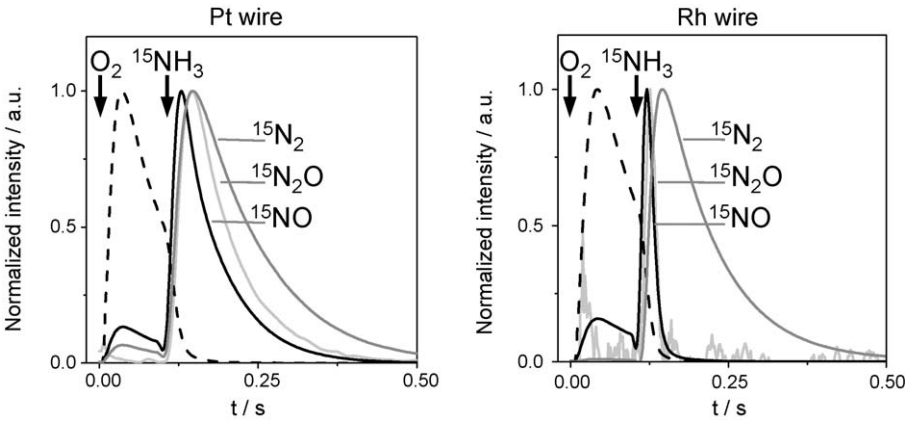

Fig. 1. Normalized transient responses of selected compounds detected over Pt and Rh wires at 1073 K in O_2:Ne = 1:1 and $^{15}NH_3$:Xe = 1:1 sequential pulse experiments with Δt = 0.1 s [30].

extrapolate the kinetics from vacuum, where TAP experiments are usually performed, to ambient pressure for describing the steady-state performance. This is an important requirement if the TAP derived kinetics should be used for optimizing reactor performance or predicting catalytic performance under conditions, where experiments cannot be easily performed. Recently, the research groups of Kondratenko and Pérez-Ramírez thoroughly investigated the direct N_2O decomposition in the TAP reactor over Rh-ZSM-5 and Fe-ZSM-5/silicalite differing in the nature of FeO_x species (isolated, oligomerized and nano-particles) [33–35]. The aim of these studies was to derive micro-kinetics of this reaction and to evaluate its potential for explaining the effect of metal and the structure of FeO_x and RhO_x species on N_2O decomposition as well as for predicting steady-state performance at ambient pressure. Fig. 2 exemplifies transient responses of N_2O, N_2 and O_2 recorded after N_2O pulsing over two selected catalytic materials. It is clearly seen that the order of appearance of N_2, and O_2 transients as well as their shapes depend on the catalyst. Analyzing the position (t_{max}) of the maximum of these responses [35], the following mechanistic concept of N_2O decomposition over Fe-containing zeolites was developed: (i) O_2 was formed slower than N_2, (ii) the higher the iron oxide clustering, the lower was the difference between the rates of O_2 and N_2 formation, (iii) no visible strong N_2O adsorption was observed and (iv) gas-phase NO was not detected. For Rh-ZSM-5, it was found that: (i) N_2 and O_2 were simultaneously formed, (ii) O_2 formation was faster than over Fe-containing catalysts, (iii) N_2O adsorbed strongly and reversibly and (iv) gas-phase NO was not formed.

Taking into account the above mechanistic knowledge, different micro-kinetic models were developed as well as quantitatively evaluated and discriminated by simultaneous fitting of the transient responses of N_2O, N_2, and O_2 [33–35]. Fig. 3 exemplifies the experimental transient responses of N_2O, N_2, and O_2 after pulsing N_2O over Fe-silicalite and Rh-ZSM-5 at 798 and 573 K, respectively. The resulting calculated responses applying the best micro-kinetic model (inserts in this figure) are shown, too. It has to be stressed that the micro-kinetic model developed for Fe-silicalite was also valid for all Fe-containing zeolites studied in [33–35]. In other words, the nature of FeO_x species (isolated, oligomerized and nano-particles) did not influence the mechanism of N_2O decomposition but affected the kinetics of individual reaction steps. There is only one reaction pathway leading to O_2, which is a complex sequence of three elementary reaction pathways (Fig. 3). The overall oxygen production and N_2O decomposition are limited by the rearrangement of an adsorbed bi-atomic oxygen species to another one. This reaction pathway is influenced by the nature of FeO_x species. The activation energy of this elementary step over isolated, oligonuclear, and FeO_x nano-particles amounted to 300, 142, and 61 kJ/mol, respectively, i.e. the FeO_x clustering facilitates the formation of gas-phase O_2. As a result the overall de-N_2O activity increases.

Despite Rh-ZSM-5 was more active for N_2O decomposition compared to Fe-containing zeolites, the activation energy of N_2O decomposition over FeO_x and RhO_x species was very similar (120–130 kJ mol^{-1} over free metal sites (*) and 83–120 kJ mol^{-1} over surface mono-atomic oxygen species (*-O)). A reason for the higher activity of RhO_x species for N_2O decomposition was found to be the pre-exponential factor (k^0) of the rate constant of N_2O decomposition, i.e. collision frequencies of N_2O with RhO_x, and FeO_x species.

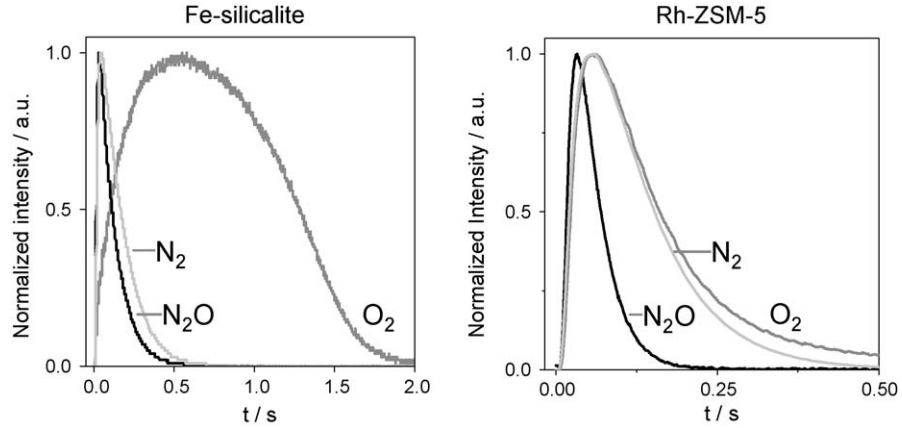

Fig. 2. Normalized transient responses of N_2O, N_2, and O_2 detected over Fe-silicalite and Rh-ZSM-5 after pulsing N_2O:Ne = 1:1 at 773 and 623 K, respectively.

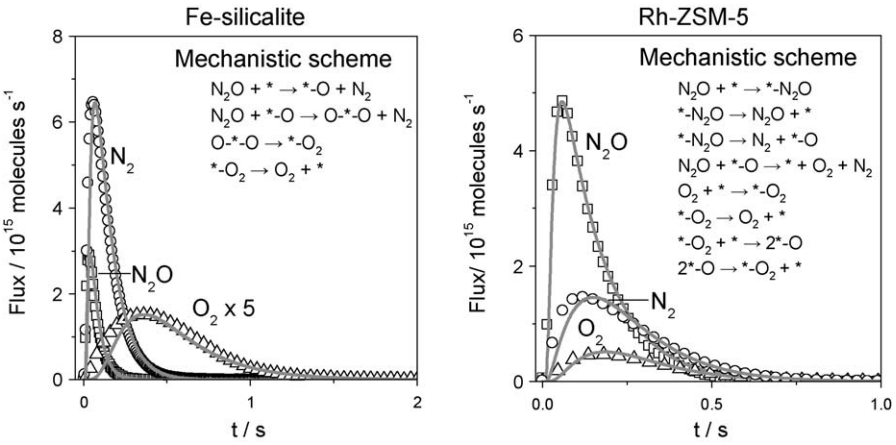

Fig. 3. Experimental and calculated transient responses of N_2, O_2 and N_2O after N_2O pulsing over Fe-silicalite and Rh-ZSM-5 at 798 and 573 K, respectively. The corresponding mechanistic schemes of N_2O decomposition are presented in the inserts.

For example, these factors for N_2O decomposition over FeO_x nanoparticles (the most active iron species), and RhO_x were $3.4 \times 10^6\ Pa^{-1}\ s^{-1}$, and $2.3 \times 10^{12}\ s^{-1}$, respectively [35]. Another key mechanistic factor determining the higher de-N_2O activity of Rh-ZSM-5 compared to Fe-containing zeolites was related to the pathways of O_2 formation. O_2 was formed over Rh-ZSM-5 via two parallel reaction pathways: (i) recombination of two active oxygen species (*-O) and (ii) direct interaction of N_2O with a surface monoatomic oxygen species (*-O). The recombination dominated above 623 K.

The obtained micro-kinetics was validated by extrapolating from vacuum to conditions of standard catalytic tests (approximately over three orders of magnitude of N_2O partial pressures) [33,35]. Both, for Fe- and Rh-containing zeolites, the respective micro-kinetic models forecasted first-order dependence of N_2O decomposition on partial pressure of N_2O and no inhibiting effect of O_2 under steady-state conditions. Moreover, they qualitatively predicted the differences in the steady-state performance of differently structured FeO_x species as well as in the de-N_2O activity of FeO_x and RhO_x species in a wide range of temperatures and N_2O partial pressures. However, the kinetics failed to quantitatively match the steady-state activity. Therefore, further thorough studies are required to identify the origins limiting the quantitative relevance of transient micro-kinetics.

3.3. *Identifying active species by time-resolved catalyst characterization*

The water–gas shift (WGS) reaction is a key step in the production of hydrogen for two large-scale industrial processes such as ammonia and methanol synthesis. This reaction is also very attractive for on-board generation of hydrogen in mobile sources. For this application, low-temperature active and stable catalysts are required. Nobel metals supported over oxides of rare earth metals are promising candidates.

From a mechanistic point of view, Iwasawa and co-worker [36] originally suggested the surface formate mechanism. Investigating surface intermediates by means of infrared spectroscopy, the group of Davis further provided consistent spectroscopic information supporting this mechanism [37–39]. It was found that CO reacted with hydrated CeO_2 yielding a surface formate species. There was also evidence from IR analysis for the formation of C–H bond when OH bonds break [40]. The rate-determining step in the formate mechanism is the decomposition of surface formate species to gas-phase hydrogen and a surface carbonate species. The latter decomposes to yield gas-phase CO_2. Kinetic measurements in [41–43] suggested also that CO can be activated over noble metals and oxidized to CO_2 by lattice oxygen of CeO_2 resulting in a reduced Ce^{3+} species. The reduced ceria was reoxidized by H_2O.

The group of Burch and Meunier in the Queen's University Belfast intensively investigated mechanistic aspects of the WGS and reversed WGS reactions over Pt- and Au-based catalysts with the aim to identify true reactive intermediates [44–47]. They developed a set-up combining in-situ diffuse reflectance infrared Fourier Transform (DRIFT) spectroscopy and on-line mass spectrometry (MS) with steady-state isotopic transient kinetic analysis [44]. The idea behind this approach was to compare the time response of isotopically labeled surface and gas-phase species by DRIFT spectroscopy and MS analysis, respectively. The results from [46] presented in Fig. 4 illustrate the importance of such analysis. Fig. 4(a) exemplifies formate and carbonate regions of steady-state DRIFT spectra obtained over (0.6 at.%Au + 7.3 at.%La)/CeO_2 after switching from $^{12}CO/H_2O/Ar = 2/7/91$ to $^{13}CO/H_2O/Ar = 2/7/91$ at 428 K. It is clearly seen that both formate and carbonate species labeled with ^{13}C were formed in the $^{13}CO/H_2O/Ar = 2/7/91$ feed. In order to conclude which surface species actively participated in the formation of gas-phase CO_2, the authors in [46] analyzed temporal changes in the IR bands of surface formates and carbonates containing ^{12}C as well as in the concentration of gas-phase $^{13}CO_2$ after switching from $^{12}CO/H_2O/Ar = 2/7/91$ to $^{13}CO/H_2O/Ar = 2/7/91$. The results are presented in Fig. 4(b). Since the temporal profiles of the carbonate and formate species were very similar, it was suggested that the exchange of these species proceeded at a similar rate. It is also obvious from Fig. 4(b) that the exchange of gas-phase CO_2 was faster than that of the surface species; the rate of CO_2 formation was ca. 60 times higher than the rate of the exchange of formate species. This quantitative evaluation indicated that the formates detected by DRIFT spectroscopy could not be the main surface intermediates of gas-phase CO_2. Similar conclusions were derived for the WGS reaction over Au(2 wt.%)/$CeZrO_4$ and Pt(2 wt.%)/CeO_2 [45]. However, the role of surface formates in the CO_2 production may change with rising temperature as demonstrated in [47]; the formate species were spectators at 433 K but became main reaction intermediates at 493 K.

Since the pioneering work of Haruta and co-workers [48], supported gold catalysts have been widely applied for the propene epoxidation [49–54]. In analogy to well-studied liquid-phase epoxidation of propene with hydrogen peroxide it was suggested that hydrogen peroxide might be also active species in the gas-phase epoxidation. However, the participation of peroxo species in this reaction was not experimentally proven. In order to elucidate the nature of active sites in the propylene epoxidation with a mixture of H_2 and O_2 over supported gold and silver catalysts, Oyama and co-workers [55–58] applied a combination of transient

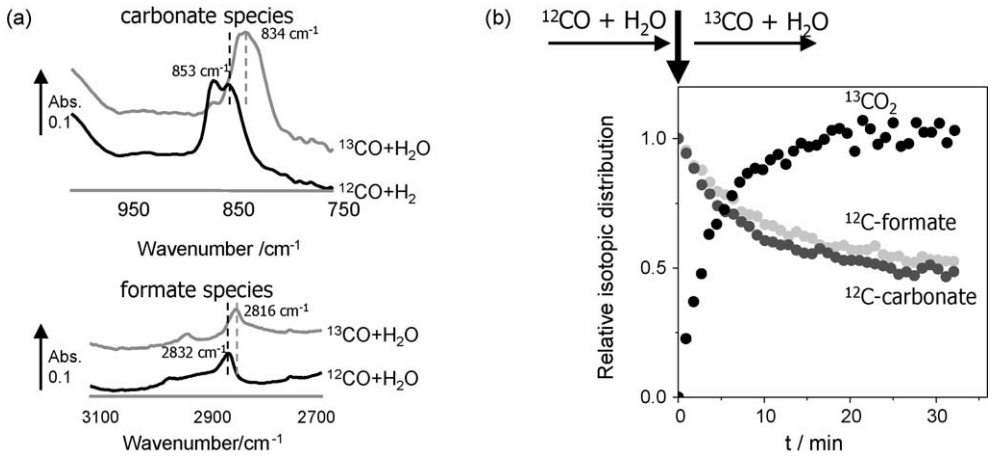

Fig. 4. Formate and carbonate DRIFT spectra (a) as well as temporal evolution of gas-phase $^{13}CO_2$ and surface ^{12}C-carbonates/^{12}C-formates (b) recorded over (0.6 at.%Au + 7.3 at.%La)/CeO_2 after switching from $^{12}CO/H_2O/Ar$ = 2/7/91 to $^{13}CO/H_2O/Ar$ = 2/7/91 at 428 K [46].

in-situ UV/vis diffuse reflectance (UV/vis-DR) spectroscopy and X-ray absorption fine structure (XAFS) spectroscopy. The formation of Ti-hydroperoxo species over Au–Ba/Ti-TUD was proven by the time-resolved in-situ UV/vis-DR spectroscopy during the oxidation of H_2 with O_2 and epoxidation of propene with H_2 and O_2 in the gas-phase. The coverage by these species was quantitatively determined from the area of the pre-edge peak in the Ti K-edge XAFS spectra under condition of propene epoxidation. Transient experiments with $H_2/O_2/Ar$ = 1/1/8 and $C_3H_6/H_2/O_2/Ar$ = 1/1/1/7 mixtures resulted in the turnover frequency (TOF) of propene epoxidation determined from temporal changes in the coverage by Ti-hydroperoxo species. This value matched the TOF value obtained from steady-state catalytic tests. Therefore, it was concluded that the Ti-hydroperoxo species formed under reaction conditions were true reactive species.

In summary, in order to unambiguously identify true active surface species, it is highly important to fully quantify not only the rates of formation of gas-phase products but also the rates of transformation of surface intermediates under the same reaction conditions. If these rates match each other, the intermediates can be considered as real active species.

3.4. Monitoring dynamics of redox processes

O_2 activation, i.e. the formation of negatively charged oxygen species from gas-phase O_2 on the catalyst surface, is an essential step for various oxidation reactions. The catalytic materials must be able to provide and accept their electrons during generation and further incorporation of oxygen species into reaction products, respectively. Therefore, it is highly important to establish the relationships between reactivity/selectivity and redox properties of catalytic materials for the rational catalyst design. Several techniques such as XRD, XANES, EPR, UV/vis-DR, Raman and IR have been developed for monitoring the redox events taking place over catalytic materials under real reaction conditions.

The UV/vis-DR spectroscopy was applied to investigate the extent of reduction of VO_x species under different reaction conditions [59–64]. However, only a few studies dealt with kinetics of reduction and reoxidation of active surface species. The kinetics of reduction of CrO_3 by CO [65] was determined from time-resolved in-situ UV/vis-DR spectroscopic analysis. Kinetic parameters of reduction of VO_x/MCM-41 by H_2 were determined from temporal changes in the range of d–d transitions of reduced VO_x species after switching from an O_2-containing flow to an H_2-containing feed [66]. Argyle et al. [62] monitored the dynamics of reduction of VO_x species over Al_2O_3 by C_3H_8 from transient analysis of UV/vis-DR spectra in the near-edge region. Redox kinetics of VO_x species in VO_x/TiO_2 catalysts used in oxidative scission of butane to acetic acid [67] was derived from in-situ UV/vis-DR spectroscopic analysis in the range of d–d transitions of reduced VO_x species.

Very recently, Ovsitser et al. [68] applied time-resolved in-situ UV/vis-DR analysis for determining kinetic parameters of reduction and oxidation of highly-dispersed VO_x species supported over $(Ti–Si)O_2$ materials by C_3H_8 and O_2/N_2O, respectively. The concentration of vanadium was amounted to 3 wt.% resulting in an apparent surface density of VO_x species of 0.4–1 V nm^{-2}, i.e. significantly below one monolayer. This study was aimed to elucidate the effect of Ti and N_2O on catalytic performance of $VO_x/(Ti–Si)O_2$ materials in the oxidative dehydrogenation of propane (ODP). The experimental set-up is shown in Fig. 5. Steady-state, time- and spatial-resolved in-situ UV/vis measurements as well as catalytic tests in combination with isotopic traces can be run simultaneously during heterogeneous catalytic gas-phase reac-

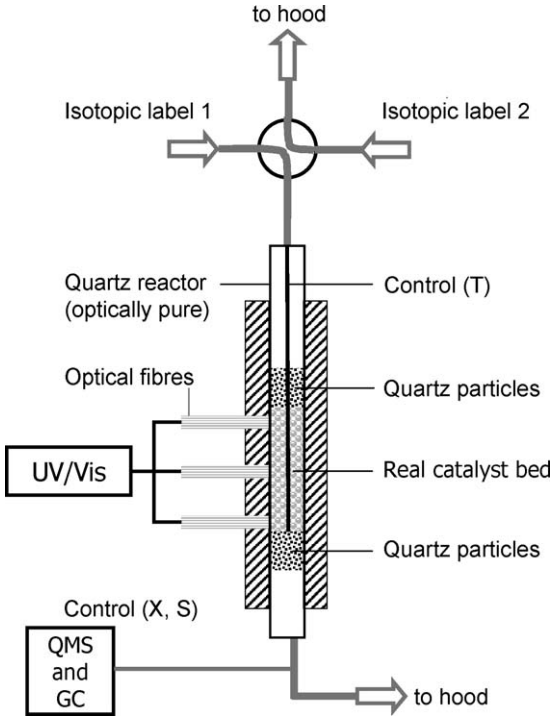

Fig. 5. Schematic representation of an in-house developed set-up for simultaneous catalytic testing and catalyst characterization by in-situ UV/vis spectroscopy.

tions from the same solid catalyst under identical reaction conditions. Kinetic parameters of reduction of oxidized VO_x species by C_3H_8 as well as reoxidation of reduced VO_x species by O_2 and N_2O were determined from quantitative analysis of temporal changes in the Kubelka–Munk function at 700 nm after switching from oxidizing (O_2/Ne = 20/80) to reducing (C_3H_8/Ne = 40/60) and back to oxidizing (O_2/Ne = 20/80 or N_2O/Ne = 40/80) feeds. These parameters are summarized in Fig. 6(a) as a function of the ratio of Ti/Si in VO_x/(Ti–Si)O_2. It is clearly seen that the constant of catalyst reduction by C_3H_8 increases with an increase in Ti loading in these samples. It is important to stress that the pure supports without VO_x species were not active for propane oxidation. This means that doping SiO_2 with Ti increased the rate of reduction of VO_x species by C_3H_8. The TOF values of C_3H_8 conversion in the steady-state ODP catalytic tests using O_2 and N_2O increased in a similar way confirming a Mars–van-Krevelen redox cycle involving lattice oxygen and reduced V^{3+} or V^{4+} centers. The presence of Ti influenced also the ratio of the constant of reoxidation of reduced VO_x species by O_2 to the constant of reoxidation by N_2O. As shown in Fig. 6(a) this ratio decreases with Ti loading. In other words, the difference in the oxidizing ability of O_2 and N_2O for the reoxidation of reduced VO_x species decreases with Ti loading.

The derived kinetic parameters were used to calculate steady-state reduction degrees of VO_x species under the ODP conditions with O_2 and N_2O assuming the Mars–van-Krevelen mechanism [68]. As shown in Fig. 6(b), the difference in these degrees between O_2 and N_2O containing feeds passes over a maximum of 0.48 at a Ti/Si ratio of 0.1 und decreases to 0.1 with a further increase in this ratio to 1.5; the smaller this difference, the closer is the reduction degree of VO_x species in the ODP reaction with O_2 and N_2O. It is important to highlight that the difference in steady-state propene selectivity (S(C3H6) with N_2O – S(C3H6) with O_2) between N_2O- and O_2-mediated ODP ($X(C_3H_8) < 2\%$, $X(N_2O) > 5\%$, $X(O_2) > 5\%$) followed the same trend as the difference in the reduction degree of VO_x species (Fig. 6(b)). Therefore, it was concluded that the reduction degree was an important selectivity-determining factor; the higher the steady-state reduction degree of VO_x species, the higher propene selectivity can be achieved. Thus, this kinetic analysis directly supported our previous suggestions on the role of the degree of catalyst reduction on ODP selectivity [69,70].

3.5. Identifying active oxygen species by steady-state isotopic transient kinetic analysis

The SSITKA technique has been widely applied in heterogeneous catalysis [13]. The main questions addressed to oxidation catalysts were: (i) the role of lattice/adsorbed oxygen species in partial oxidation, (ii) mobility of lattice oxygen species and (iii) determining the number of active sites responsible for the formation of oxidation products. The latter is usually complicated by readsorption of these products.

Lemonidou and co-workers [71,72] applied the SSITKA technique in order to understand why ethylene selectivity in the oxidative dehydrogenation of ethane (ODE) over Ni-Nb-O mixed catalysts was significantly improved when Nb was incorporated into NiO. They analyzed the distribution of ^{16}O and ^{18}O isotopic labels in gas-phase oxygen, carbon dioxide and water after switching from $^{16}O_2$/Ar/He = 1/2/97 to $^{18}O_2$/He = 1/99 and from $^{16}O_2/C_2H_6$/Ar/He = 1/1/2/96 to $^{18}O_2/C_2H_6$/He = 1/1/98. Analyzing the temporal profiles of $^{16}O^{18}O$, and $^{16}O_2$ [72], these authors concluded that: (i) the adsorption of gas-phase oxygen was dissociative and irreversible and (ii) the presence of Nb in NiO decreased the amount and the mobility of exchangeable oxygen species in their catalyst as well as suppressed the formation of electrophilic oxygen species, like O^-, O_2^-, and O_2^{2-}. From the analysis of $C^{16}O_2$, $C^{16}O^{18}O$, $C^{18}O_2$, $H_2{}^{16}O$, and $H_2{}^{18}O$ transients, it was suggested that strongly bonded lattice O^{2-} species was responsible for selective dehydrogenation of ethane to ethylene, while nonstoichiometric O^- species participated in direct oxidation of ethane to carbon dioxide.

In a very recent study, Nijhuis et al. [73] investigated propene epoxidation over Au(1 wt.%)/TiO_2 and Au(1 wt.%)/Ti-SBA-15 with H_2 and O_2 using the SSITKA technique. The aim was to prove whether oxygen of supporting material is involved in the mechanism of propene epoxidation. Their results indicated that the support provided its oxygen for product formation. At least two different pathways were suggested for the formation of carbon dioxide. These routes differed in the amount of oxygen available for the reaction and were related to nanometer and sub-nanometer gold particles. However, the authors in [73] did not obtain unambiguous insights into the role of lattice oxygen in the formation of propene oxide.

Our previous studies on the ODP reaction over differently loaded VO_x/γ-Al_2O_3 [69] and VO_x/SiO_2 [64,70] as well as individual vanadium oxides (V_2O_3, VO_2, and V_2O_5) [63] demonstrated that C_3H_6 selectivity was significantly improved when the reaction was performed with N_2O instead of O_2. Understanding the origin(s) of the superior selective performance of N_2O compared to O_2 may help to identify selective and non-selective processes with the aim to design catalytic materials performing selectively with O_2, too. To this end, we performed a detailed mechanistic analysis on the role of oxygen species in the ODP applying the TAP reactor, the SSITKA technique and DFT calculations [64,74,75].

Mechanistic insights into the role of oxygen species from VO_x species and from gas-phase O_2 in CO_2 formation were derived from

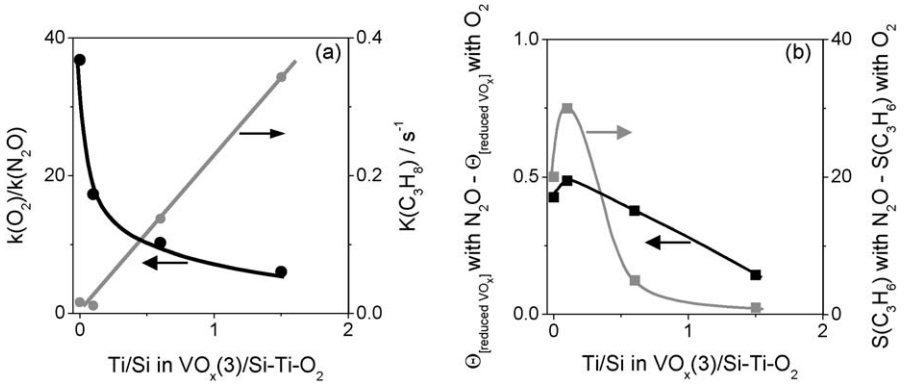

Fig. 6. Kinetic parameters of reduction (by C_3H_8) and reoxidation (by O_2, and N_2O) of VO_x over VO_x(3 wt.%)/(Ti–Si)O_2 materials (a). Differences in the coverage by reduced VO_x species and in the propene selectivity in the ODP reaction with N_2O and O_2 over VO_x(3 wt.%)/(Ti–Si)O_2 materials (b). Reaction conditions: T = 773 K, C_3H_8:O_2:Ne = 40:20:40, C_3H_8:N_2O:Ne = 40:40:20.

the analysis of temporal profiles of $C^{16}O_2$, $C^{18}O^{16}O$, and $C^{18}O_2$ formed over $V^{16}O_x(5)$/MCM-41 and $V_2{}^{16}O_5$ at 773 K upon switching from a C_3H_8:$^{16}O_2$:Ar:Ne = 4:2:92:2 mixture to a C_3H_8:$^{18}O_2$:Ar:Ne = 4:2:92:2 mixture. Since non-labeled oxygen ($^{16}O_2$) was not present in the latter feed but $C^{16}O_2$ and $C^{18}O^{16}O$ were observed, it was concluded that lattice oxygen of VO_x species participated in the formation of carbon dioxide. The analysis of statistical distribution of ^{16}O and ^{18}O in differently labeled carbon dioxides suggested that oxygen species responsible for the formation of carbon dioxide were not chemically equivalent [75], i.e. there existed differently active oxygen species. Some ideas on the nature of oxygen species responsible for the formation of C_3H_6 and CO_x from C_3H_8, were derived from DFT calculations of O_2 and N_2O interactions with reduced VO_x species and of C_3H_8 and C_3H_6 interactions with surface oxygen species formed from O_2 and N_2O [74]. These calculations predicted the formation of peroxovanadates as precursors of vanadyl species upon reoxidation of reduced VO_x species with O_2 but not with N_2O. The peroxovanadates species were highly reactive for consecutive propene oxidation to CO_x. Based on this combined experimental and theoretical study as well as on the kinetic analysis of reduction and oxidation of VO_x species in Section 3.4, the following selectivity-governing factors in the ODP reaction were determined: (i) density of surface lattice oxygen species; the lower the density the higher the selectivity and (ii) the presence of non-lattice adsorbed oxygen species, which are not selective. These properties can be tuned by the support as well as by the nature of VO_x species and oxidizing agents.

4. Summary and outlook

The examples discussed above illustrate the enormous potential of time-resolved methods for studying mechanistic aspects of various heterogeneous oxidation reactions. Since one or several parameters are changed during one transient experiment in a broader range compared to one steady-state experiment, more detailed reaction kinetics can be, therefore, derived from transient analysis. Transient experiments with sub-millisecond time resolution and their micro-kinetic evaluation open the possibility to unravel complex catalytic reactions on a near to elementary level. However, due to the complexity of quantitative evaluation of time-resolved experiments, there is still need for developments in numerical tools for full kinetic analysis of gas-phase and surface species at a level of near to elementary reaction steps. An important issue, which is rarely tackled in transient kinetic analysis, is the relevance of transient kinetics for predicting steady-state performance.

Combining time-resolved in-situ catalyst characterization techniques with transient isotopic analysis in one unit enables: (i) to directly monitor the nature of active surface species under real reaction conditions, (ii) to simply derive kinetic parameters of transformation of active surface intermediates and (iii) to derive insights into the nature of oxygen species participating in selective and non-selective reactions.

For the TAP reactor, it is anticipated that modern fibre optic spectroscopies like UV/vis and Raman can be integrated for controlling possible changes in the composition of reducible oxides under operating vacuum conditions. A closer relationship between the catalyst status and kinetic parameters could be established. However, in order to directly relate changes in the catalyst compositions with transients of gas-phase species in TAP experiments, the time resolution of characterization techniques has still to be improved.

Combining time-resolved analysis of gas-phase and surface species with their spatial-resolved characterization down to nanometer range will significantly increase the potential of transient technique for the molecular understanding of catalytic reactions. This would make possible to directly relate the structural information with micro-kinetic one. The same experimental approach can be also applied for analyzing gas–solid systems at evaluated pressures and liquid-phase reactions. In addition to monitoring catalytic events, it is also advantageous to combine time- and spatial-resolved characterization techniques for watching processes occurring during preparation and activation of catalytic materials.

References

[1] G. Ertl, H. Knözinger, F. Schüth, J. Weitkamp (Eds.), Handbook of Heterogeneous Catalysis, Wiley-VCH, Weinheim, 2008.
[2] J.M. Thomas, Angew. Chem. Int. Ed. 38 (1999) 3588.
[3] J.M. Thomas, C.R.A. Catlow, G. Sankar, Chem. Commun. (2002) 2921.
[4] J.F. Haw, in: J.F. Haw (Ed.), In-situ Spectroscopy in Heterogeneous Catalysis, Wiley-VCH, Weinheim, 2002.
[5] B.M. Weckhuysen, Phys. Chem. Chem. Phys. 5 (2003) 4351.
[6] B.M. Weckhuysen (Ed.), In-situ Spectroscopy of Catalysts, American Scientific Publishers, 2004.
[7] M.A. Banares, Catal. Today 100 (2005) 71.
[8] B.C. Gates, H. Knözinger (Eds.), Adv. Catal., Elsevier, 2007.
[9] B.M. Weckhuysen, Angew. Chem. Int. Ed. 48 (2009) 4910.
[10] J.T. Gleaves, J.R. Ebner, T.C. Kuechler, Catal. Rev. Sci. Eng. 30 (1988) 49.
[11] J.T. Gleaves, G.S. Yablonskii, P. Phanawadee, Y. Schuurman, Appl. Catal. A 160 (1997) 55.
[12] J. Pérez-Ramírez, E.V. Kondratenko, Catal. Today 121 (2007) 160.
[13] S.L. Shannon, J.J.G. Goodwin, Chem. Rev. 95 (1995) 677.
[14] H. Kobayashi, K. Kobayashi, Catal. Rev. 10 (1975) 139.
[15] C.O. Bennett, Catal. Rev. Sci. Eng. 13 (1976) 121.
[16] P.L. Mills, J.J. Lerou, Rev. Chem. Eng. 9 (1993) 1.
[17] A.T. Bell, L.L. Hegedus (Eds.), Catalysis under Transient Conditions, American Chemical Society, Washington, DC, 1982.
[18] J. Happel, Isotopic Assessment of Heterogeneous Catalysis, Academic Press, New York, 1986.
[19] P. Szedlacsek, L. Guczi (Eds.), Appl. Catal. A 151 (1997) 1.
[20] R.J. Berger, F. Kapteijn, J.A. Moulijn, G.B. Marin, J. De Wilde, M. Olea, D. Chen, A. Holmen, L. Lietti, E. Tronconi, Y. Schuurman, Appl. Catal. A 342 (2008) 3.
[21] J.R. Ebner, J.T. Gleaves, US4626412, 1986.
[22] J.R. Ebner, J.T. Gleaves, EP0266334, 1988.
[23] J.T. Gleaves, US5376335, 1994.
[24] J.T. Gleaves, US5500371, 1996.
[25] J. Perez-Ramirez, E.V. Kondratenko, V.A. Kondratenko, M. Baerns, J. Catal. 227 (2004) 90.
[26] J. Perez-Ramirez, E.V. Kondratenko, Chem. Commun. (2004) 376.
[27] J. Perez-Ramirez, E.V. Kondratenko, V.A. Kondratenko, M. Baerns, J. Catal. 229 (2005) 303.
[28] M. Baerns, V.A. Kondratenko, R. Kraehnert, R. Imbihl, A. Scheibe, W.K. Offermans, R.A. Van Santen, J. Catal. 232 (2005) 226.
[29] J. Perez-Ramírez, E.V. Kondratenko, J. Catal. 250 (2007) 240.
[30] J. Perez-Ramírez, E.V. Kondratenko, G. Novell-Leruth, J.M. Ricart, J. Catal. 261 (2009) 217.
[31] R. Imbihl, A. Scheibe, Y.F. Zeng, S. Gunther, R. Kraehnert, V.A. Kondratenko, M. Baerns, W.K. Offermans, A.P.J. Jansen, R.A. van Santen, Phys. Chem. Chem. Phys. 9 (2007) 3522.
[32] E.V. Kondratenko, J. Perez-Ramirez, Appl. Catal. A 289 (2005) 97.
[33] E.V. Kondratenko, J. Pérez-Ramírez, J. Phys. Chem. B 110 (2006) 22586.
[34] E.V. Kondratenko, J. Pérez-Ramírez, Catal. Today 121 (2007) 197.
[35] E.V. Kondratenko, V.A. Kondratenko, M. Santiago, J. Pérez-Ramírez, J. Catal. 256 (2008) 248.
[36] T. Shido, Y. Iwasawa, J. Catal. 141 (1993) 71.
[37] G. Jacobs, L. Williams, U.M. Graham, G.A. Thomas, D.E. Sparks, B.H. Davis, Appl. Catal. A 252 (2003) 107.
[38] G. Jacobs, P.M. Patterson, U.M. Graham, A.C. Crawford, A. Dozier, B.H. Davis, J. Catal. 235 (2005) 79.
[39] G. Jacobs, S. Ricote, B.H. Davis, Appl. Catal. A 302 (2006) 14.
[40] G. Jacobs, B.H. Davis, Appl. Catal. A 284 (2005) 31.
[41] T. Bunluesin, R.J. Gorte, G.W. Graham, Appl. Catal. B 15 (1998) 107.
[42] Q. Fu, A. Weber, M. Flytzani-Stephanopoulos, Catal. Lett. 77 (2001) 87.
[43] S. Hilaire, X. Wang, T. Luo, R.J. Gorte, J. Wagner, Appl. Catal. A 215 (2001) 271.
[44] D. Tibiletti, A. Goguet, F.C. Meunier, J.P. Breen, R. Burch, Chem. Commun. (2004) 1636.
[45] F.C. Meunier, A. Goguet, C. Hardacre, R. Burch, D. Thompsett, J. Catal. 252 (2007) 18.
[46] F.C. Meunier, D. Reid, A. Goguet, S. Shekhtman, C. Hardacre, R. Burch, W. Deng, M. Flytzani-Stephanopoulos, J. Catal. 247 (2007) 277.
[47] F.C. Meunier, D. Tibiletti, A. Goguet, S. Shekhtman, C. Hardacre, R. Burch, Catal. Today 126 (2007) 143.
[48] T. Hayashi, K. Tanaka, M. Haruta, J. Catal. 178 (1998) 566.
[49] B.S. Uphade, Y. Yamada, T. Akita, T. Nakamura, M. Haruta, Appl. Catal. A 215 (2001) 137.

[50] G. Mul, A. Zwijnenburg, B. van der Linden, M. Makkee, J.A. Moulijn, J. Catal. 201 (2001) 128.
[51] A.K. Sinha, S. Seelan, T. Akita, S. Tsubota, M. Haruta, Appl. Catal. A 240 (2003) 243.
[52] T.A.R. Nijhuis, T. Visser, B.M. Weckhuysen, Angew. Chem. Int. Ed. 44 (2005) 1115.
[53] T.A. Nijhuis, T. Visser, B.M. Weckhuysen, J. Phys. Chem. B 109 (2005) 19309.
[54] B. Chowdhury, J.J. Bravo-Suarez, N. Mimura, J.Q. Lu, K.K. Bando, S. Tsubota, M. Haruta, J. Phys. Chem. B 110 (2006) 22995.
[55] J.J. Bravo-Suarez, J. Lu, C.G. Dallos, T. Fujitani, S.T. Oyama, J. Phys. Chem. C 111 (2007) 17427.
[56] J.Q. Lu, X.M. Zhang, J.J. Bravo-Suarez, K.K. Bando, T. Fujitani, S.T. Oyama, J. Catal. 250 (2007) 350.
[57] J.Q. Lu, X.M. Zhang, J.J. Bravo-Suarez, S. Tsubota, J. Gaudet, S.T. Oyama, Catal. Today 123 (2007) 189.
[58] J.J. Bravo-Suarez, K.K. Bando, J.I. Lu, M. Haruta, T. Fujitani, S.T. Oyama, J. Phys. Chem. C 112 (2008) 1115.
[59] X. Gao, M.A. Bañares, I.E. Wachs, J. Catal. 188 (1999) 325.
[60] X. Gao, J.-M. Jehng, I.E. Wachs, J. Catal. 209 (2002) 43.
[61] M.D. Argyle, K. Chen, C. Resini, K.C.A.T. Bell, E. Iglesia, J. Phys. Chem. B 108 (2004) 2345.
[62] M.D. Argyle, K. Chen, E. Iglesia, A.T. Bell, J. Phys. Chem. B 109 (2005) 2414.
[63] E.V. Kondratenko, O. Ovsitser, J. Radnik, M. Schneider, R. Kraehnert, U. Dingerdissen, Appl. Catal. A 319 (2007) 98.
[64] O. Ovsitser, M. Cherian, E.V. Kondratenko, J. Phys. Chem. C 111 (2007) 8594.
[65] A. Bensalem, B.M. Weckhuysen, R.A. Schoonheydt, J. Phys. Chem. B 101 (1997) 2824.
[66] G. Grubert, J. Rathousky, G. Schulz-Ekloff, M. Wark, A. Zukal, Microporous Mesoporous Mater. 22 (1998) 225.
[67] U. Bentrup, A. Brückner, M. Fait, B. Kubias, J.B. Stelzer, Catal. Today 112 (2006) 78.
[68] O. Ovsitser, M. Cherian, A. Brückner, E.V. Kondratenko, J. Catal. 265 (2009) 8.
[69] E.V. Kondratenko, M. Baerns, Appl. Catal. A 222 (2001) 133.
[70] E.V. Kondratenko, M. Cherian, M. Baerns, D.S. Su, R. Schlogl, X. Wang, I.E. Wachs, J. Catal. 234 (2005) 131.
[71] E. Heracleous, A.A. Lemonidou, J. Catal. 237 (2006) 162.
[72] E. Heracleous, A.A. Lemonidou, J. Catal. 237 (2006) 175.
[73] T.A. Nijhuis, E. Sacaliuc-Parvulescu, N.S. Govender, J.C. Schouten, B.M. Weckhuysen, J. Catal. 265 (2009) 161.
[74] X. Rozanska, E.V. Kondratenko, J. Sauer, J. Catal. 256 (2008) 84.
[75] O. Ovsitser, E.V. Kondratenko, Catal. Today 142 (2009) 138.